J. Phys. Chem. Solids Vol. 50, No. 4, pp. 347–352, 1989
Printed in Great Britain.

0022-3697/89 $3.00 + 0.00

# $^{31}$P SOLID STATE NMR STUDIES OF ZrP, $Mg_3P_2$, $MgP_4$ AND $CdPS_3$

R. A. Nissan and T. A. Vanderah
Chemistry Division, Research Department, Naval Weapons Center, China Lake, CA 93555, U.S.A.

(*Received* 21 *March* 1988; *accepted* 17 *October* 1988)

**Abstract**—The $^{31}$P solid state NMR spectra of ZrP, $Mg_3P_2$, $MgP_4$, and $CdPS_3$ are reported. Static and magic-angle-spinning (MAS) spectra were obtained for each compound. In all cases, chemical shift anisotropy and the effects of dipolar broadening were sufficiently reduced by the MAS method to reveal the isotropic chemical shifts for each crystallographically distinct phosphorus. The observed resonances were assigned to the different types of phosphorus by considering the structural details of each compound. In ZrP the two chemical shifts of +128.4 and +187.5 ppm (relative to 85% $H_3PO_4$) were assigned to P occupying the Wyckoff 2*d* and 2*a* sites, respectively. In $Mg_3P_2$, two resonances from the 24*d* and 8*a* site P atoms were observed at −262.3 and −239.6 ppm, respectively. In $MgP_4$ two types of phosphorus, one type coordinated to two Mg and two P and the other to three P and one Mg, gave chemical shifts of −109.2 and −6.1 ppm, respectively. From $CdPS_3$ only one resonance at +104.9 ppm is observed as all P atoms are crystallographically equivalent.

*Keywords:* P-31 MAS NMR, $Mg_3P_2$, solid state NMR, $MgP_4$, ZrP, $CdPS_3$.

## INTRODUCTION

The development of magic-angle-spinning nuclear magnetic resonance (MAS NMR) spectroscopy has greatly facilitated multinuclear studies of solid state samples. Review texts [1, 2] and articles [3, 4] have appeared which discuss the methods in detail.

Liquid state NMR spectra are characterized by sharp resonances with clearly discernible isotropic chemical shifts: on the NMR time scale, molecular tumbling is fast and produces "motional narrowing"—an averaging of various line-broadening effects arising from interactions of the nuclei with other nuclei and with electric field gradients due to anisotropic chemical environments. In contrast, the absence of Brownian motion in solids as well as the extended nature of the chemical bonding make them predisposed to severe line-broadening effects, and line-narrowing techniques such as MAS must be used to obtain well defined NMR spectra.

Under MAS conditions, the equations describing most of the line-broadening interactions in solids depend on the term $3\cos^2\theta - 1$, where $\theta$ is the angle between the applied magnetic field and the axis about which the sample is spinning. This term vanishes at $\theta = 54.7°$ (the magic angle). Therefore, if the sample is rotated about an axis inclined 54.7° to the applied magnetic field, most broadening effects are reduced to zero since all nuclei have been effectively placed on this axis by the process of rapid spinning about it. MAS also averages the orientation-dependent contributions to the chemical shielding and reveals the solution-like isotropic chemical shift. The chemical shift anisotropy, which can be observed in the shapes of the broad resonances obtained under non-spinning conditions, is a measure of the asymmetry of the electric field surrounding the nucleus under investigation. If the sample spinning frequency is less than the line width of the chemical shift anisotropy, part of the resonance signal is displaced into spinning sidebands which flank the isotropic signal; the chemical shift values of the sidebands differ from that of the isotropic signal by multiples of the spinning frequency.

Application of MAS NMR to the characterization of solids is particularly important in cases where X-ray diffraction is of limited utility; e.g. the aluminosilicates, such as zeolites, which are often poorly crystalline in addition to requiring differentiation between Al and Si, which differ by only one atomic number. Numerous $^{29}$Si and $^{27}$Al MAS NMR studies on this class of compounds [4–6] have demonstrated the usefulness of the method in elucidating local structural environments.

The $^{31}$P nucleus ($S = 1/2$) has a natural abundance of 100% and is easily probed by NMR. Extensive solution state $^{31}$P NMR studies have been carried out on biological and organic systems [7] and on organometallic phosphine derivatives [8–10]. Reports have recently appeared on solid state studies of inorganic phosphates [4, 11], pyrophosphates [12], and phosphate glasses [4, 13]. Non-molecular inorganic phosphorus-containing compounds have been the least studied, although reports have appeared on sphalerite-type InP and GaP [14], chalcopyrite-type $ZnSnP_2$ [15], and the chalcopyrite-type series $ZnSiP_2$, $ZnGeP_2$, and $ZnSnP_2$ [16].

At the present time, theoretical calculations of chemical shift value in $^{31}$P NMR spectra are not possible [4, 7]. $^{31}$P resonance positions are extremely

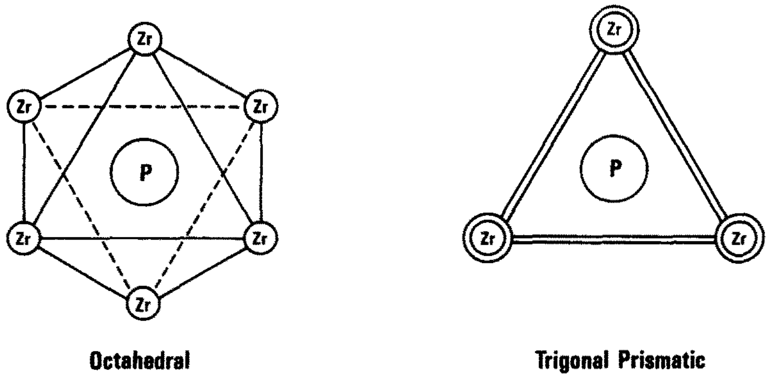

Fig. 1. Coordination geometries of phosphorus in ZrP; octahedral: 2*a* site, trigonal prismatic: 2*d* site.

sensitive to a variety of complex and interrelated factors such as the variation of the hybridization of phosphorus, which may involve *s*, *p*, and *d* orbital contributions, inductive factors due to chemical bond type, local coordination geometry, and formal oxidation state. Much of the recent work on MAS NMR of solids has therefore involved structurally and chemically well characterized compounds in order to establish qualitative relationships and an interpretative data base which might be extended to less well characterized samples. We report here the $^{31}P$ solid state NMR spectra and detailed structural discussions of the non-molecular inorganic solids ZrP, $Mg_3P_2$, $MgP_4$, and $CdPS_3$.

## EXPERIMENTAL METHODS

Hexagonal ZrP was obtained commercially (CERAC, 99.5%). Attempts to obtain the cubic form from this commercial product by quenching in liquid nitrogen from 1025°C were not successful. Loss of phosphorus is necessary to stabilize cubic ZrP [17, 18]; therefore, $ZrP_{0.92}$ was prepared from stoichiometric amounts of the elements which were ground together, sealed in an evacuated silica ampule, and heated at 800–900°C for two days. After cooling over 24 h to room temperature, only the hexagonal phase was detectable by X-ray diffraction; however, after reheating at 1100°C for 12 h and quenching in liquid nitrogen, the cubic form was clearly present in the X-ray diffraction pattern, although 80–90% of the sample retained the hexagonal structure. $Mg_3P_2$ was obtained commercially (Pfaltz & Bauer). $MgP_4$ was prepared as a byproduct in the attempted synthesis of $MgGeP_2$ [19]. $CdPS_3$ crystals were grown from the elements [20].

Samples were identified by X-ray diffraction (Cu K$\alpha$ radiation) using a Scintag PAD V powder diffractometer, the Gandolfi method for crystals, and/or the Debye–Scherrer method.

$^{31}P$ NMR spectra were obtained with an NT-200 WB spectrometer equipped with a magic-angle-spinning probe. The probe was tuned to 81 MHz and an external sample of 85% phosphoric acid was used as the reference standard. Samples were ground and packed into a 7 mm diameter rotor and spun at 3–5 kHz. Non-spinning spectra were also recorded. When sample quantities were limited, approx. 5 mg of the compound was mixed with KBr prior to loading. Spectra were acquired by a one-pulse method using a 30° pulse and a 10 s recycle time. Spectra were usually obtained in an hour or less, but experiments involving small amounts of material or broad resonances required overnight data acquisitions.

## RESULTS AND DISCUSSION

### ZrP

Hexagonal ZrP adopts a structure with space group $P6_3/mmc$ ($a = 3.684$, $c = 12.554$ Å) [18, 21]. Zr atoms occupy the Wyckoff 4*f* positions while the P atoms are equally distributed in the 2*a* and 2*d* sites. The structure can be described using close-packing terminology: phosphorus atoms form hexagonally close-packed layers in the sequence, along the *c*-axis, *ABCB*. Zirconium atoms occupy all octahedral sites between the P layers. The structure can therefore be thought of as interpenetrating slabs of NaCl-like (*ABC*) and NiAs-like (*BCB*) sandwiches. The coordination of phosphorus by zirconium alternates along the *c*-axis from octahedral (2*a* site) in the NaCl-like slabs to trigonal prismatic (2*d* site) in the NiAs-like slabs. The two different coordination geometries of phosphorus are depicted in Fig. 1. The two types of phosphorus are clearly distinguished in the $^{31}P$ NMR spectra shown in Fig. 2. The static spectrum shows partial resolution of the two axially symmetric resonances which are of comparable intensity, as expected from the equal distribution of phosphorus in the two crystallographic sites. Spinning at the magic angle resolves the resonances, revealing the isotropic signals *A* and *B* at +128.4 and +187.5 ppm, respectively. The sample spinning frequency, however, is considerably less than the chemical shift anisotropy which is reflected in the intensities of the spinning sidebands $a_1$ to $a_4$ and $b_1$ to $b_4$. In order to assign the resonances to the

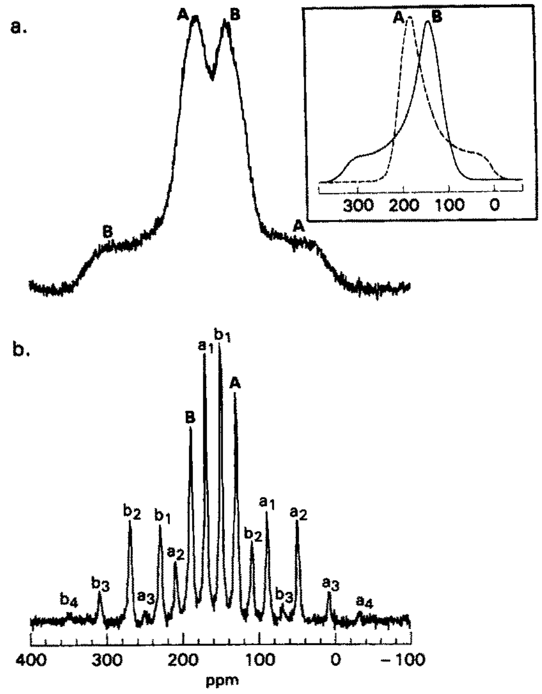

Fig. 2. Solid state $^{31}P$ NMR spectra of hexagonal ZrP. (a) Static spectrum; inset depicts the shapes of the two axially symmetric resonances. (b) MAS spectrum; the isotropic signals $A$ and $B$ are flanked by first- to fourth-order spinning sidebands $a_1$ to $a_4$ and $b_1$ to $b_4$, respectively.

different types of phosphorus, the $^{31}P$ MAS NMR spectrum of the cubic form of ZrP, which has the NaCl structure and therefore only octahedrally coordinated phosphorus, was sought. The $^{31}P$ NMR spectra of $ZrP_{0.92}$, which exhibited 10–20% conversion to the cubic form and therefore enrichment in octahedral phosphorus, are shown in Fig. 3. Enhancement of the downfield $B$ signal at +187.5 ppm is seen in the MAS spectrum and this resonance is assigned to octahedral phosphorus. The downfield position of the signal may be related to a greater number of 90° bonding interactions, which are associated with large downfield shifts of $^{31}P$ NMR signals in organometallic phosphine-derived systems [8–10]. In octahedral coordination the Zr–P–Zr bond angles are either 90° (twelve) or 180° (three). In the trigonal prismatic site the Zr–P–Zr bond angles, calculated from the reported interatomic distances [18], are 91.6° (six), 137.2° (six), and 72.8° (three). In both coordination sites the Zr–P bond lengths are 2.643 Å [18].

## $Mg_3P_2$

$Mg_3P_2$ adopts the cubic anti-bixbyite structure [22, 23]. Numerous sesquioxides, including many of the rare earth elements, exhibit the cubic bixbyite structure. The anti-bixbyite structure of $Mg_3P_2$ is derived from the cubic bixbyite structure of the metal sesquioxides by switching the metal and non-metal positions: magnesium occupies the oxygen position and phosphorus the metal position. There are 16 formula weights per unit cell ($Ia3$, $a = 12.01$ Å); the 48 Mg atoms are located in the Wyckoff 48$e$ site, and the 32 P atoms fill the 8$a$ and 24$d$ sites. Therefore, two crystallographically different types of phosphorus are present in a ratio of 1:3. Both phosphorus positions are six-coordinate by Mg, as illustrated in Fig. 4 [24]. The overall structure is related to that of fluorite, $CaF_2$, in which the coordination of Ca is cubic. The bixbyite structure is obtained by removing one-fourth of the fluoride ions and allowing all the atom positions to shift slightly. At the former Ca sites, or P sites in $Mg_3P_2$, there are now six-coordinate positions of two types. Each is derived from a cubic arrangement by removing two of eight vertices. For one-fourth of the positions (8$a$ site) these two are at the ends of a body diagonal, and for the remainder (24$d$ site) at the ends of a face-diagonal, as shown in Fig. 4. The Mg atoms are four-coordinate by P in approximately regular tetrahedra. The $^{31}P$ NMR spectra of $Mg_3P_2$ are given in Fig. 5. The chemical shift anisotropy is evident in the asymmetric non-spinning spectrum, but is greatly reduced in the MAS spectrum which reveals two isotropic chemical shifts $A$ and $B$ at −262.3 and −239.6 ppm, respectively. The relative intensities are in agreement with the 1:3 crystallographic distribution of phosphorus. The upfield and more intense

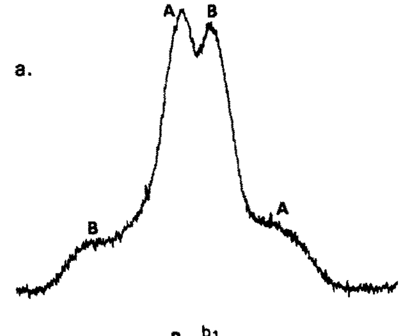

Fig. 3. Solid state $^{31}P$ NMR spectra of $ZrP_{0.92}$ which are a mixture of cubic and hexagonal forms of ZrP. (a) Static spectrum. (b) MAS spectrum; isotropic signals $A$ and $B$ are flanked by spinning sidebands $a_1$ to $a_3$ and $b_1$ to $b_3$, respectively; signal $A$ is assigned to trigonal prismatic phosphorus (2$d$ site) and $B$ to octahedral phosphorus (2$a$ site).

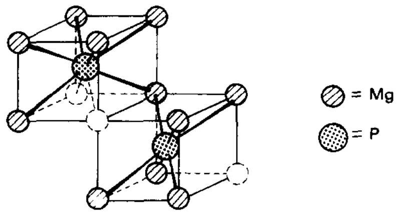

Fig. 4. Coordination geometries of phosphorus in anti-bixbyite-type $Mg_3P_2$; both the 24*d* and the 8*a* sites are six-coordinate and are derived from cubic eight-coordination by removing two vertices.

signal *A* is assigned to three-fourths of the P atoms which occupy the 24*d* site; the less intense and downfield signal *B* arises from those occupying the 8*a* site. The bond lengths and angles about P were calculated from the published crystallographic data [22]. For the 8*a* site the P–Mg bond lengths are equivalent at 2.649 Å; the Mg–P–Mg bond angles are 74.4° (six), 105.6° (six), and 180° (three). For the 24*d* site the P–Mg bond lengths are 2 at 2.555, 2 at 2.577, and 2 at 2.604 Å; the bond angles are 76.6° (six), 94.1° (one), 102.7° (two), 110.6° (two), 112.8° (one), 130.4° (one), and 169.5° (two). The bond lengths in the 24*d* site are significantly shorter than those in the 8*a* site. This may account for increased shielding of phosphorus because of its closer approach to the electropositive metals; however, the differences in bond angles indicate differences in the hybridization of phosphorus which could be equally important.

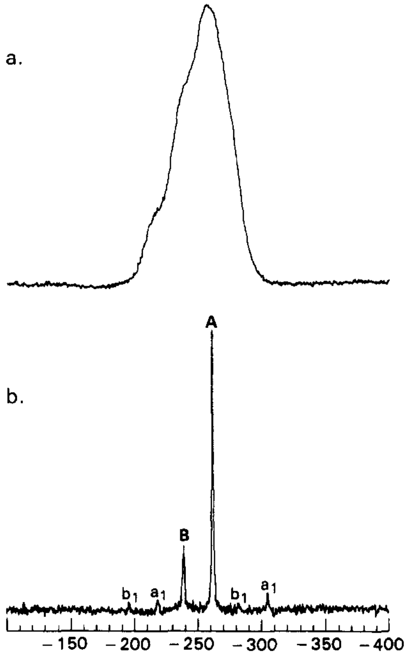

Fig. 5. Solid state $^{31}P$ NMR spectra of $Mg_3P_2$. (a) Static spectrum. (b) MAS spectrum; isotropic signals *A* and *B* are flanked by first-order spinning sidebands $a_1$ and $b_1$; relative intensities assign *A* to the 24*d* site and *B* to the 8*a* site.

Two $^{31}P$ solid state NMR studies of $Mg_3P_2$ have been reported previously [25, 26]. The spectrum obtained in the present study is consistent with the results of Kessemeier and Norberg [25], who also reported two resonances separated by 24 ppm; however, Gibby *et al.* [26] reported an additional broad resonance 225 ppm downfield.

## $MgP_4$

This compound is isotypic to $CdP_4$ and crystallizes in the monoclinic space group $P2_1/c$ ($a = 5.144$, $b = 5.085$, $c = 7.526$ Å, $\beta = 98.66°$, $Z = 2$ formula weights per unit cell) [27]. The two Mg atoms per unit cell occupy the Wyckoff 2*a* sites while the eight P atoms are equally divided into two sets of general 4*e* positions. Each phosphorus is pseudo-tetrahedral, one type ($P_1$) is bonded to two Mg and two P at 2.608, 2.635, 2.184, and 2.185 Å, respectively, with bond angles 114.3°, 101.6°, 120.1°, 105.7°, 108.9°, and 105.2° [27]. The other type of phosphorus ($P_2$) is bonded to one Mg and three P at 2.862, 2.184, 2.185, and 2.252 Å, respectively, with bond angles 96.2°, 102.7°, 109.9°, 111.3°, 111.5°, and 124.2° [27]. Each Mg is coordinated to six P. A projection of the structure on the (010) plane of the unit cell is depicted in Fig. 6; $MgP_4$ is a Zintl phase containing infinite polyanionic chains of catenated phosphorus. The solid state $^{31}P$ NMR spectra of $MgP_4$ are given in Fig. 7. Two asymmetric $^{31}P$ resonances of comparable intensity are observed in the static spectrum, as expected from equal numbers of phosphorus in the two coordination sites. The spinning spectrum resolves the two isotropic chemical shifts *A* and *B* at −109.2 and −6.1 ppm, respectively. The upfield resonance *A* arising from the P atom with greater shielding is assigned to $P_1$ which is bonded to two metallic atoms, in contrast to $P_2$ which is bonded to only one metal. Since there is considerable P–P bonding in $MgP_4$, significant P–P homonuclear dipole–dipole broadening might be expected. However, the isotropic signals at *A* and *B* are relatively narrow, indicating that MAS at moderate spinning speeds is very effective in reducing this broadening effect. For example, the expected dipole–dipole

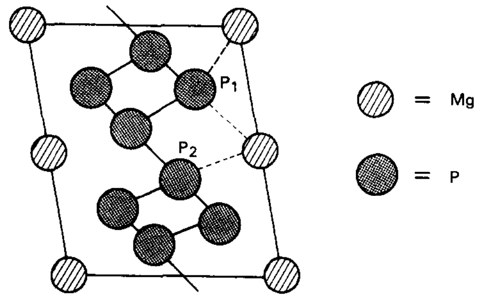

Fig. 6. Projection of the $MgP_4$ structure on the (010) plane of the unit cell [25]; $P_1$ is bonded to two Mg and two P, $P_2$ to three P and one Mg.

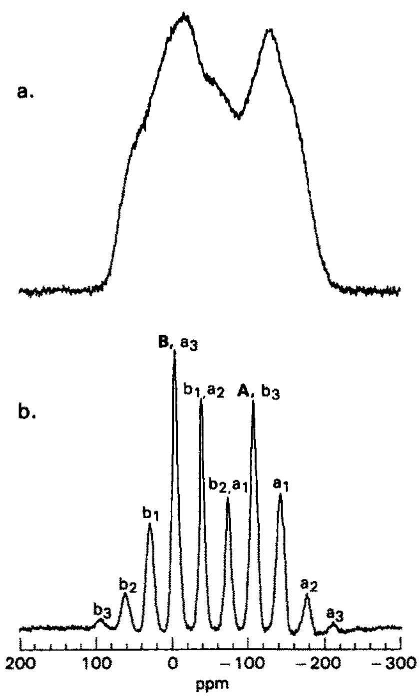

Fig. 7. Solid state $^{31}$P NMR spectra of $MgP_4$. (a) Static spectrum. (b) MAS spectrum; isotropic signals $A$ and $B$ are flanked by spinning sidebands $a_1$ to $a_3$ and $b_1$ to $b_3$, sideband $b_1$ overlaps with $a_2$ and $b_2$ with $a_1$; signal $A$ is assigned to $P_1$ and $B$ to $P_2$.

broadening of two protons separated by 2 Å is approx. 10 kHz [1]. This is reduced by a factor of six for two $^{31}$P nuclei at the same separation because of the relative magnetogyric ratios of $^1$H and $^{31}$P [1].

## $CdPS_3$

$CdPS_3$ is considered to be a layered thiophosphate containing $(P_2S_6)^{4-}$ clusters [28, 29]. The structure can be derived from that of cubic, two-dimensional $CdCl_2$: one can consider a close-packed sulfur array with all octahedral sites filled in every other layer. In $CdCl_2$, Cd fills these octahedral sites but in $CdPS_3$ they are half-filled by Cd and half by P–P units, and distortions lower the symmetry to monoclinic ($C2/m$; $a = 6.218(1)$, $b = 10.763(2)$, $c = 6.867(1)$ Å, $\beta = 107.58(1)°$; $Z = 4$ formula weights per unit cell) [30]. All phosphorus atoms are crystallographically equivalent and occupy the Wyckoff $4i$ position. The sulfur atoms are of two types, one-third occupying another set of $4i$ sites, with the remainder in the $8j$ general positions. Cadmium atoms occupy the $4g$ sites. The local geometry about phosphorus is shown in Fig. 8 [29]. Each P is four-coordinate to three S and one P, with bond lengths of 2.032(2) and 2 at 2.027(1) Å to sulfur, and 2.222(2) Å to phosphorus [30]. The local geometry about P is therefore pseudo-tetrahedral, and its chemical behavior indicates a positive formal valence, in contrast to that in ZrP, $Mg_3P_2$, and $MgP_4$. The $^{31}$P solid state NMR spectra are shown in Fig. 9. The MAS spectrum reveals a single isotropic resonance $A$ as expected since all phosphorus atoms are crystallographically equivalent. As in $MgP_4$, the narrowness of the isotropic signal at +109.4 ppm indicates that MAS has effectively removed any P–P homonuclear dipole–dipole broadening which would arise from the P–P bonding in $CdPS_3$.

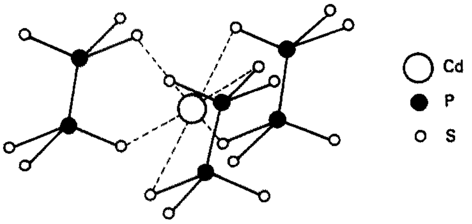

Fig. 8. Coordination geometry about phosphorus in $CdPS_3$; P atoms are part of $(P_2S_6)^{4-}$ clusters; all are crystallographically equivalent and four-coordinate to three S and one P.

## CONCLUSIONS

The $^{31}$P MAS NMR spectra of ZrP, $Mg_3P_2$, $MgP_4$, and $CdPS_3$ indicate that crystallographically different phosphorus atoms can be distinguished. Different degrees of chemical anisotropy about phosphorus are

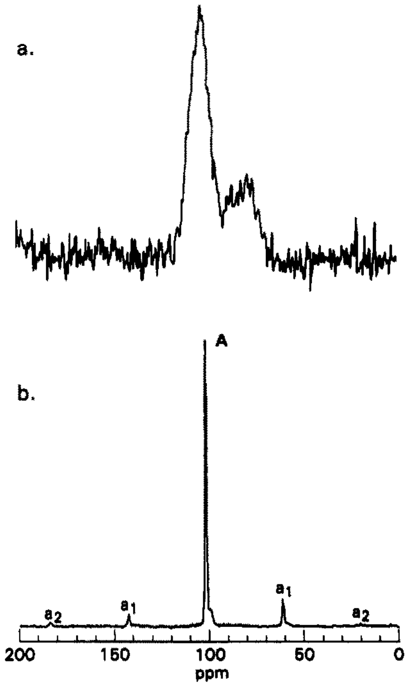

Fig. 9. Solid state $^{31}$P NMR spectra of $CdPS_3$. (a) Static spectrum. (b) MAS spectrum; one isotropic signal is observed with first- and second-order spinning sidebands; the shoulder observed is due to chemical shift anisotropy or an impurity not detectable by X-ray diffraction.

Table 1. $^{31}$P MAS NMR summary

| Compound | Signal† | $\delta$ (ppm)‡ | Site§ | Comments |
|---|---|---|---|---|
| ZrP | *A*<br>*B* | +128.4<br>+187.5 | 2*d*<br>2*a* | Two isotropic chemical shifts; large CSA¶ |
| $Mg_3P_2$ | *A*<br>*B* | −262.3<br>−239.6 | 24*d*<br>8*a* | Two isotropic shifts in a ratio of 3:1 |
| $MgP_4$ | *A*<br>*B* | −109.2<br>−6.1 | 4*e*<br>4*e* | Two isotropic shifts; large CSA |
| $CdPS_3$ | *A* | +104.9 | 4*i* | One isotropic shift; large CSA |

† See spectra.

‡ Chemical shift relative to 85% $H_3PO_4$.

§ Wyckoff crystallographic notation for phosphorus position(s); see text and figures.

¶ Chemical shift anisotropy.

reflected in the broad, asymmetric shapes of the static spectra. The isotropic chemical shifts revealed in the MAS spectra were assigned to crystallographically different phosphorus sites by considering the structural details of each compound.

*Acknowledgements*—The authors thank Roxanne Quintana for assistance in obtaining the NMR spectra, David Decker for carrying out the synthesis of $ZrP_{0.92}$, and Dr Charlotte Lowe-Ma for helpful structural discussions and computation of the bond angles in $Mg_3P_2$. The comments of Prof. Gregory Geoffroy of Pennsylvania State University are much appreciated. This work was supported by the Office of Naval Research and the Naval Air Systems Command.

## REFERENCES

1. Fyfe C. A., *Solid State NMR for Chemists*. C.F.C. Press, Ontario (1983).
2. Fukushima A. and Roeder S. B. W., *Experimental Pulse NMR*. Addison-Wesley, Reading, Massachusetts (1981).
3. O'Donnell D. J., Bartuska V. J., Palmer A. R. and Sindorf D. W., *Am. Lab.* **18:96** (1986).
4. Turner G. L., Kirkpatrick R. J., Risbud S. H. and Oldfield E., *Am. Ceram. Soc. Bull.* **66,** 656–663 (1987).
5. Thomas J. M., Fyfe C. A., Ramdas S., Klinowski J. and Gobbl G. C., *J. phys. Chem.* **86,** 3061, and references cited therein (1982).
6. Klinowski J., Thomas J. M. Fyfe C. A. and Hartman J. S., *J. phys. Chem.* **85,** 2590, and references cited therein (1981).
7. Mavel G., In *Annual Reports on NMR Spectroscopy* (Edited by E. F. Mooney), Vol. 5B. Academic Press, New York (1973).
8. Carty A. J., Maclaughlin S. A. and Taylor N. J., *J. Organometallic Chem.* **204,** C27–C32 (1981).
9. Petersen J. L. and Stewart R. P., Jr, *Inorg. Chem.* **19,** 186, (1981).
10. Garrou P. E., *Chem. Rev.* **81,** 229 (1981).
11. Jakeman R. J. B., Cheetham A. K., Clayden N. J. and Dobson C. M., *J. Am. chem. Soc.* **107,** 6249 (1985).
12. Mudrakovskii I. L., Shmachkova V. P., Kotsarenko N. S. and Mastikhin V. M., *J. Phys. Chem. Solids* **47,** 335 (1986).
13. Villa M., Carduner K. R. and Chiodelli G., *J. Solid St. Chem.* **69,** 19 (1987).
14. Duncan T. M., Karlicek R. F., Jr, Bonner W. A. and Thiel F. A., *J. Phys. Chem. Solids* **45,** 389 (1984).
15. Ryan M. A., Peterson M. W., Williamson D. L., Frey J. S., Maciel G. E. and Parkinson B. A., *J. Mater. Res.* **2,** 528 (1987).
16. Vanderah T. A. and Nissan R. A., *J. Phys. Chem. Solids* **49,** 1335 (1988).
17. Schoenberg N., *Acta chem. scand.* **8,** 226 (1954).
18. Irani K. S. and Gingerich K. A., *J. Phys. Chem. Solids* **24,** 1153 (1963).
19. Hewston T. A., *J. Solid St. Chem.* **69,** 179 (1987).
20. Covino J., Dragovich P., Lowe-Ma C. K., Kubin R. F. and Schwartz R. W., *Mater. Res. Bull.* **20,** 1099 (1985).
21. Wyckoff R. W. G., *Crystal Structures*, 2nd edn, Vol. 1, pp. 146–148. Interscience, New York (1963).
22. Stackelberg M. V. and Paulus R., *Z. phys. Chem.* **22B,** 305 (1933).
23. Ref. 21, Vol. 2, pp. 2–6.
24. Wells A. F., *Structural Inorganic Chemistry*, 4th edn p. 451. Clarendon, Oxford (1933).
25. Kessemeier H. and Norberg R. E., *Phys. Rev.* **155,** 321 (1967).
26. Gibby M. G., Pines A., Rhim W. K. and Waugh J. S., *J. chem. Phys.* **56,** 991 (1972).
27. Schnering H. G. von and Menge G. Z., *anorg. allg. Chem.* **422,** 219 (1976).
28. Ohno Y. and Hirama K., *J. Solid St. Chem.* **63,** 258 (1986).
29. Mercier H., Mathey Y. and Canadell E., *Inorg. Chem.* **26,** 963 (1987).
30. Ouvrard G., Brec R. and Rouxel J., *Mater. Res. Bull.* **20,** 1181 (1985).